ELECTRONIC MATERIALS 5

Physical Models of Semiconductor Quantum Devices

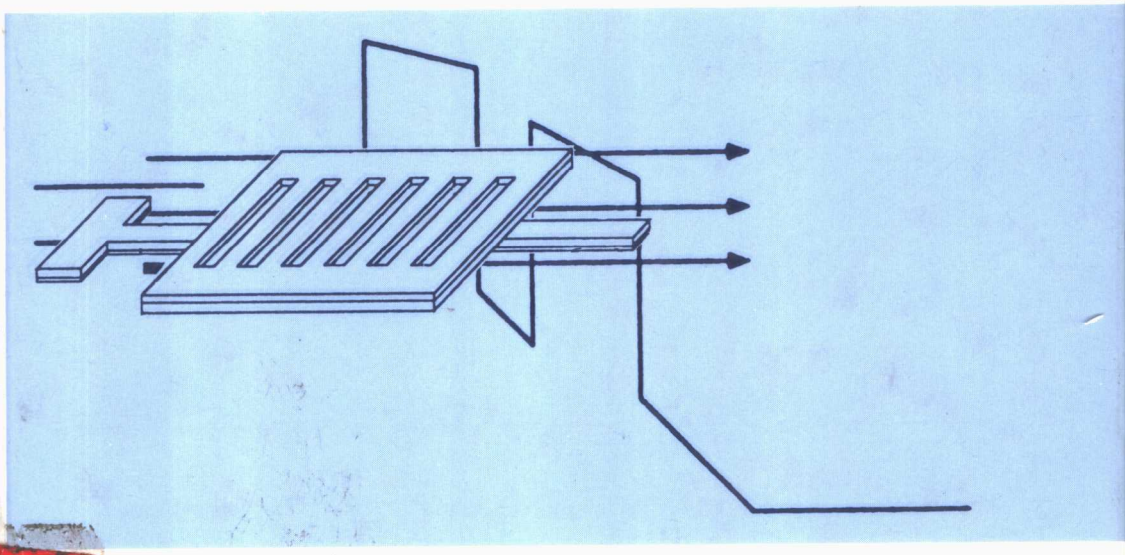

ig Fu and Magnus Willander

KLUWER ACADEMIC PUBLISHERS

Physical Models of Semiconductor Quantum Devices

By

Ying Fu
Gothenburg University
And
Chalmers University of Technology

Magnus Willander
Gothenburg University
And
Chalmers University of Technology

KLUWER ACADEMIC PUBLISHERS
Boston/Dordrecht/London

Distributors for North, Central and South America:
Kluwer Academic Publishers
101 Philip Drive
Assinippi Park
Norwell, Massachusetts 02061 USA
Telephone (781) 871-6600
Fax (781) 871-6528
E-Mail <kluwer@wkap.com>

Distributors for all other countries:
Kluwer Academic Publishers Group
Distribution Centre
Post Office Box 322
3300 AH Dordrecht, THE NETHERLANDS
Telephone 31 78 6392 392
Fax 31 78 6546 474
E-Mail <orderdept@wkap.nl>


Electronic Services <http://www.wkap.nl>

Library of Congress Cataloging-in-Publication Data

Fu, Ying, 1964
Physical models of semiconductor quantum devices / by Ying Fu, Magnus Willander.
p. cm. -- (Electronic materials series : 5)
Includes index.
ISBN 0-7923-8457-1
1. Semiconductors. 2. Semiconductors--Materials.
3. Optoelectronics. I. Willander, M. II. Title. III. Series.
QC610.9.F8 1999
537.6'22--dc21 99-11907
CIP

Printed on acid-free paper.

Printed in the United States of America

PREFACE

Solid state electronics is undergoing rapid changes driven by heteroepitaxy, lithography, and new device concepts. While ten years ago Si was the material of choice in solid state electronics, now GaAs, InGaAs ,AlAs,InP, Ge,etc. have all become quite important. The advent of semiconductor lasers and integrated optoelectronic circuits has led to a flurry of activities in compound semiconductors. Additionally, the remarkable advances in the thin film epitaxy have allowed active semiconductor devices with sub-three-dimensional properties and built-in controlled biaxial strain due to lattice mismatch.

This book addresses three main areas of interest: i) electronic and optical properties of low-dimensional semiconductor materials: ii) principal physics of quantum electronic devices, iii) principal physics of quantum optical devices. These areas will provide readers with an intimate knowledge of the new material properties on which novel solid state electronic devices such as quantum diode, and small size transistor, high electron mobility transistor are based, leading to the very front of the development of material and device research. The link between basic physics on which the real devices are based and the output from the real devices is closely observed in the book.

Contents

Chapter 1

Elemental and compound semiconductors

1.1 Crystalline nature of solids

The intrinsic property of a crystal is that the environment around a given atom or group of atoms is exactly the same as the environment around another atom or similar group of atoms. To understand and to define the crystal structure, two important concepts are introduced, i.e., the lattice and the basis.

The *lattice* represents a set of points in the space which form a periodic structure. Each point sees exactly the same environment. A building block of atoms, called the *basis*, is then attached to each lattice point, yielding a crystal structure.

An important property of a lattice is the ability to define three vectors, $\mathbf{a}_1$, $\mathbf{a}_2$, and $\mathbf{a}_3$, such that any lattice point $\mathbf{R}'$ can be obtained from any other lattice point $\mathbf{R}$ by a translation

$$\mathbf{R}' = \mathbf{R} + m_1\mathbf{a}_1 + m_2\mathbf{a}_2 + m_3\mathbf{a}_3 \ , \tag{1.1}$$

where m_1, m_2, and m_3 are three integers. The translation vectors, $\mathbf{a}_1$, $\mathbf{a}_2$, and $\mathbf{a}_3$ are called primitive if the volume of the cell formed by them is the smallest possible.

There are 14 types of lattices in three dimensional space. We shall focus on the cubic lattice which is the structure taken by all semiconductors. There are three kinds of cubic lattices: simple cubic, body-centered cubic and face-centered cubic. The simple cubic lattice is generated by the prim-

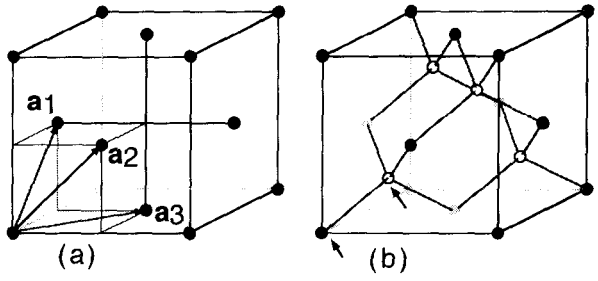

Figure 1.1: (a) Face-centered cubic lattice. (b) The zincblende crystal structure.

itive vectors of $\mathbf{a}_1 = a\mathbf{x}_0$, $\mathbf{a}_2 = a\mathbf{y}_0$, and $\mathbf{a}_3 = a\mathbf{z}_0$, where $\mathbf{x}_0$, $\mathbf{y}_0$, and $\mathbf{z}_0$ are the three unit vectors of a normal rectangular Cartesian coordinate.

The *face-centered cubic Bravais lattice* (fcc) (see Fig. 1.1): To construct the fcc lattice we add to the simple cubic lattice an additional point in the center of each square face. The fcc Bravais lattice is of great importance, since an enormous variety of solids crystalise in this form with an atom (or ion) at each lattice site.

Essentially all semiconductors of interest for electronics and optoelectronics have the fcc structure. However, they have two atoms per basis. The coordinates of the two basis atoms are (000) and $(a/4)(111)$ (indicated in Fig. 1.1b by two arrows). If the two atoms of the basis are identical, the structure is called the diamond structure. Semiconductors such as silicon, germanium and carbon fall into this category. If the two atoms are different, for examples, GaAs, AlAs, CdS, the structure is called zincblende.

Semiconductors with the diamond structure are often called elemental semiconductors, while the zincblende semiconductors are usually called compound semiconductors. The compound semiconductors are also denoted by the positions of the atoms in the periodic table, for examples GaAs, AlAs and InP are called III-V semiconductors while CdS, CdSe and CdTe are called II-VI semiconductors.

Many of the properties of crystals and many of the theoretical techniques used to describe crystals derive from the periodicity of crystalline structures. This suggests the use of Fourier analysis as an analytical tool. In the analysis of periodic time varying fields (for examples, the acoustic signal analysis and radio signal analysis) we often do much of the analytical work in the frequency domain rather than in the time domain. In analogy with the time–frequency duality, there is a corresponding *real space–reciprocal space* or *wave vector space* duality for crystal problem discussions. Many

concepts are best understood in terms of functions of the *wave vector*. We prefer to describe a wave with wavelength λ as a plane wave with wave vector $\mathbf{k}$ of magnitude $2\pi/\lambda$ and propagation direction perpendicular to the wave front. The space of the wave vectors is called the reciprocal space, the analogue of the frequency domain for the time problem.

A simple transformation is carried out to map the real space lattice into the reciprocal space ($\mathbf{k}$-space)

$$\begin{aligned}
\mathbf{b}_1 &= 2\pi \frac{\mathbf{a}_2 \times \mathbf{a}_3}{\mathbf{a}_1 \cdot \mathbf{a}_2 \times \mathbf{a}_3} , \\
\mathbf{b}_2 &= 2\pi \frac{\mathbf{a}_3 \times \mathbf{a}_1}{\mathbf{a}_1 \cdot \mathbf{a}_2 \times \mathbf{a}_3} , \\
\mathbf{b}_3 &= 2\pi \frac{\mathbf{a}_1 \times \mathbf{a}_2}{\mathbf{a}_1 \cdot \mathbf{a}_2 \times \mathbf{a}_3} .
\end{aligned} \tag{1.2}$$

A general vector

$$\mathbf{G} = m_1\mathbf{b}_1 + m_2\mathbf{b}_2 + m_3\mathbf{b}_3 \tag{1.3}$$

is called a reciprocal lattice vector, where the m_1, m_2 and m_3 are three integers (either positive or negative). It is worth noting the special relation

$$\exp(i\mathbf{G} \cdot \mathbf{R}) = 1 , \tag{1.4}$$

where $\mathbf{R}$ is a lattice vector in Eq. (1.1) but often called the direct lattice vector to distinguish it from the reciprocal lattice vector.

So far we have discussed crystal structures that are present in natural semiconductors. These structures are the lowest free energy configuration of the solid state of the atoms. Since the electrical and optical properties of the semiconductors are completely determined by the crystal structures, artificial structures, e.g., heteromaterials (among them the well-known superlattices have been fabricating even since mid-1970s inspired by the pioneering work of Esaki and Tsu at IBM) grown by heteroepitaxial crystal growth techniques such as molecular beam epitaxy (MBE) and metal-organic chemical vapor deposition (MOCVD) have made a tremendous impact on the semiconductor physics, the semiconductor technology and the semiconductor electronic and optoelectronic device industry.

Since the new heteroepitaxial techniques allow one to grow heterostructures with atomic control, one can change the periodicity of the crystal in the growth direction. This leads to the concept of superlattices where two (or even more) semiconductors A and B are grown alternately with thickness d_A and d_B respectively. The periodicity of the superlattice in the growth direction is then $d_A + d_B$. An AlGaAs/GaAs quantum well grown by molecular beam epitaxy is illustrated in Fig. 1.2. Superlattices that have been grown can be placed in three general categories: i) lattice matched, ii) latticed strained, and iii) lattice strained with intermediate substrate.

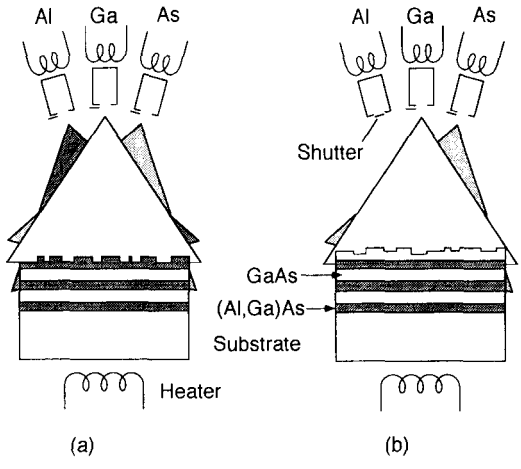

Figure 1.2: Schematic diagram illustrating the growth of a AlGaAs/GaAs multiple quantum well by MBE. Deposition of (a) (Al,Ga)As, (b) GaAs. The system is under high vacuum.

1.2 Electrons in solids

We start with the real space Schrödinger equation for a periodic lattice structure

$$\left[\frac{-\hbar^2\nabla^2}{2m} + V(\mathbf{r})\right]\psi(\mathbf{r}) = E\psi(\mathbf{r}) \ , \tag{1.5}$$

where the first term represents the kinetic energy and $V(\mathbf{r})$ is the periodic potential energy

$$V(\mathbf{r}+\mathbf{R}) = V(\mathbf{r}) \ , \tag{1.6}$$

where $\mathbf{R}$ is any lattice vector.

The Bloch theorem states that the solutions of the Schrödinger equation of Eq. (1.5) with periodic condition of Eq. (1.6) have the following properties

$$\begin{aligned} &\psi_{n\mathbf{k}}(\mathbf{r}) = \frac{1}{\sqrt{N}} u_{n\mathbf{k}}(\mathbf{r}) e^{i\mathbf{k}\cdot\mathbf{r}} \ , \\ &u_{n\mathbf{k}}(\mathbf{r}) = u_{n\mathbf{k}}(\mathbf{r}+\mathbf{R}) \ , \\ &\int_{\text{cell}} d\mathbf{r}\, u^*_{n\mathbf{k}}(\mathbf{r}) u_{n\mathbf{k}}(\mathbf{r}) = 1 \ , \end{aligned} \tag{1.7}$$

and $E = E_n(\mathbf{k})$ is the energy dispersion relationship. Here $N = N_x N_y N_z$, N_x is the number of unit cells in the crystal along the x-direction, n is the

Table 1.1: Atomic structures.

	IV semiconductors		III-V semiconductors
Si	$1s^2s^22p^6\mathbf{3s^23p^2}$	Ga	$1s^22s^22p^63s^2sp^63d^{10}\mathbf{4s^24p^1}$
Ge	$1s^22s^22p^63s^23p^63d^{10}\mathbf{4s^24p^2}$	As	$1s^22s^22p^63s^2sp^63d^{10}\mathbf{4s^24p^3}$

energy band index and $\hbar\mathbf{k}$ is the quasi-momentum of the crystal electron which will be discussed later together with the derivation of Eqs. (1.9). Here we have imposed periodic boundary conditions on the wavefunction

$$\psi(\mathbf{r}) = \psi(\mathbf{r} + N_x\mathbf{a}_x) \ . \tag{1.8}$$

Applying an external force $\mathbf{F}$, e.g., due to an external electromagnetic field $(\mathbf{E}, \mathbf{B})$,

$$\begin{aligned} \hbar\dot{\mathbf{k}} &= \mathbf{F} = -e\left(\mathbf{E} + \frac{1}{c}\mathbf{v}\times\mathbf{B}\right) \ , \\ \mathbf{v} &= \frac{1}{\hbar}\frac{\partial E}{\partial \mathbf{k}} \ . \end{aligned} \tag{1.9}$$

Here $-e$ is the electron charge and $\mathbf{v}$ is the electron group velocity.

Before further examining the various properties of semiconductors it is extremely useful to examine the atomic structure of some of the elements which make up the various semiconductor as listed in the following table, Table 1.1.

A very important conclusion can be drawn about the elements making up the semiconductors: The outmost valence electrons are made up of electrons in either the s- or p-type orbitals. While this conclusion is strictly true for elements in the atomic form, it turns out that even in the crystalline semiconductors the electrons in the valence and conductor band retain this s- or p-type character. The core electrons are usually not of interest as will be later on, except of some special characterization-type experiments.

As the atoms of the elements making up the semiconductors are brought together to form the crystal, the valence electronic states are perturbed by the presence of neighboring atoms. While the original atomic functions describing the valence electrons are, of course, no longer eigenstates of the problem, they can be used as a good approximate set of basis states to describe the "crystalline" electrons. This motivates the tight-binding method.

For most semiconductor materials of interest, the atomic functions required to describe the outermost electrons are the s, p_x, p_y, and p_z types. Moreover, since there are two atoms per basis in a semiconductor, we then

require ten functions to describe the central cell part of the Bloch functions in the form of

$$\Psi(\mathbf{r}) = \sum_{\mathbf{R}_i} \sum_{m=1}^{5} \sum_{j=1}^{2} C_{mj}(\mathbf{k}) \psi_{mj}(\mathbf{r} - \mathbf{r}_j - \mathbf{R}_i) e^{i\mathbf{k}\cdot\mathbf{R}_i} , \tag{1.10}$$

where the sum over $\mathbf{R}_i$ runs over all unit cells, m is the index of the different atomic functions ψ_{mj} used in the basis, and j denotes the atoms in each unit cell.

Once the expansion set for the crystal states has been chosen, the coefficients C_{mj} remain to be determined. To this end, the Schrödinger equation is in the form of a secular determinant

$$|\langle \psi_{m'j'} | H - E | \Psi(\mathbf{k}, \mathbf{r}) \rangle| = 0 , \tag{1.11}$$

where H is the Hamiltonian of the system under investigation.

In theory, one can calculate the matrix elements in the secular determinant, Eq. (1.11), by determining the crystal potential. This however is very difficult because of the complexity of the problem. Slater and Koster were the first to advocate the use of the tight-binding method as an empirical technique. In their formalism, the matrix elements of the secular determinant are treated as disposable constants. Energy levels in the band structure can be obtained and fitted with the measurement data by adjusting the disposable constants.

For semiconductors of device application interest, i.e., cubic semiconductors with both diamond (silicon and germanium) and zincblende symmetries (III-V group), we shall discuss the conduction band and valence band.

The conduction band consists of three sets of band minima located at the Γ_{15}-point at $\mathbf{k} = 0$, the L-points at $\mathbf{k} = (\pi/a, \pi/a, \pi/a)$, and along the Δ lines from $(0,0,0)$ to $(\pi/a, 0, 0)$, from $(0,0,0)$ to $(0, \pi/a, 0)$, and from $(0,0,0)$ to $(0,0,\pi/a)$, where a is the lattice constant. The valence band tops are located at Γ_{15}. Two bands are normally degenerate at this point, i.e., the HH and LH bands; the third one is the spin-split-off band due to the spin-orbital interaction. Figure 1.3 shows the energy band structure of carbon and silicon calculated by the sp^3s^* tight-binding model [1].

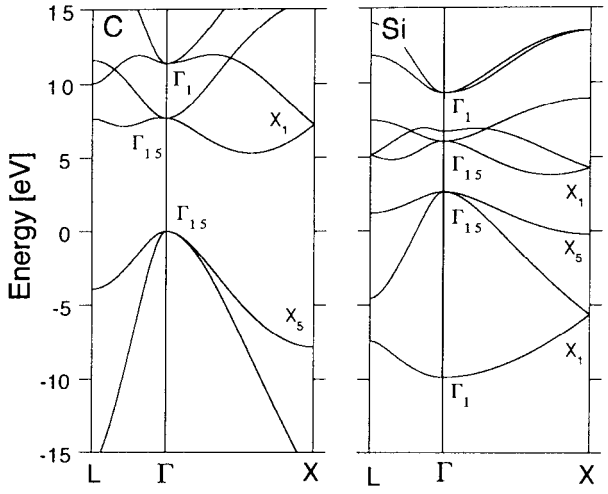

Figure 1.3: Energy band structures of diamond-structure carbon and silicon calculated by the sp^3s^* tight-binding model.

1.2.1 Conduction band

In the region around an energy minimum at $\mathbf{k}_0$ in the conduction band, the energy dispersion relationship $E(\mathbf{k})$ can be expressed as

$$E(\mathbf{k}) = E(\mathbf{k}_0) + \sum_i \frac{\partial E}{\partial k_i}(k_i - k_{0,i}) + \sum_{ij} \frac{\partial^2 E}{\partial k_i \partial k_j}(k_i - k_{0,i})(k_j - k_{0,j}) + \dots , \tag{1.12}$$

where $i, j = x, y, z$. The linear terms vanish because of the spatial invariance under translation of $\mathbf{k} \to -\mathbf{k}$. In the region around $\mathbf{k}_0$ where the higher orders can be neglected, the energy dispersion $E(\mathbf{k})$ is approximated by a quadratic function of $\mathbf{k}$:

$$E(\mathbf{k}) = E(\mathbf{k}_0) + \sum_{ij} \frac{\hbar^2}{2} \left(\frac{1}{m}\right)_{ij} (k_i - k_{0,i})(k_j - k_{0,j}) ,$$
$$\left(\frac{1}{m^*}\right)_{ij} = \frac{1}{\hbar^2} \left[\frac{\partial^2 E(\mathbf{k})}{\partial k_i \partial k_j}\right]_{\mathbf{k}=\mathbf{k}_0} . \tag{1.13}$$

Here $(1/m^*)_{ij}$ is the effective-mass tensor.

1. Spherical band:

$$E(\mathbf{k}) = E(\mathbf{k}_0) + \frac{\hbar^2(\mathbf{k}-\mathbf{k}_0)^2}{2m^*} \ . \tag{1.14}$$

2. Ellipsoidal band:

$$E(\mathbf{k}) = E(\mathbf{k}_0) + \frac{\hbar^2}{2}\left[\frac{(\mathbf{k}_l-\mathbf{k}_{0,l})^2}{m_l^*} + \frac{(k_t-k_{0,t})^2}{m_t^*}\right] \ , \tag{1.15}$$

where $\mathbf{k}_l$ and k_t are longitudinal and transverse components of wave vector $\mathbf{k}$, m_l^* and m_t^* are longitudinal and transverse effective masses.

1.2.2 Valence band

The valence band is much more complicated than the conduction band because of the intermixing among the heavy hole, light hole and spin-split-off bands. The $\mathbf{k}\cdot\mathbf{p}$ perturbation Hamiltonian in the form of

$$\frac{\hbar\mathbf{k}\cdot\mathbf{p}}{m^*}$$

is widely used to describe the valence band, where m^* is the carrier effective mass. We choose a basis of $|x\uparrow\rangle$, $|y\uparrow\rangle$, $|z\uparrow\rangle$, $|x\downarrow\rangle$, $|y\downarrow\rangle$, and $|z\downarrow\rangle$, where x, y, and z denote the three orbitals associated with Γ_{15}' representation of the top of the valence band and $\uparrow$ and $\downarrow$ denote spin up and down. By the usual perturbation theory, the wavefunction and the energy are power series in $\mathbf{k}$:

$$\begin{aligned}
\psi_\alpha &= |\alpha 0\rangle + \sum_i k_i\psi_i^{\alpha 1} + \sum_{ij} k_ik_j\psi_{ij}^{\alpha 2} + \\
&+ \sum_{ijm} k_ik_jk_m\psi_{ijm}^{\alpha 3} + \sum_{ijmn} k_ik_jk_mk_n\psi_{ijmn}^{\alpha 4} + \cdots \ , \\
E_\alpha &= E^{\alpha 0} + \sum_i k_iE_i^{\alpha 1} + \sum_{ij} k_ik_jE_{ij}^{\alpha 2} + \sum_{ijm} k_ik_jk_mE_{ijm}^{\alpha 3} + \\
&+ \sum_{ijmn} k_ik_jk_mk_nE_{ijmn}^{\alpha 4} + \cdots \ ,
\end{aligned} \tag{1.16}$$

where $|\alpha\rangle$ is one of the six basis orbitals. Superscript $\alpha 0, \alpha 1 \ldots$ denote the order of correction to the wavefunction and energy. $E^{\alpha 0}$ is the valence band edge and is usually set as the zero energy reference point. $E_i^{\alpha 1}$, $E_{ijm}^{\alpha 3}$ and other odd-order corrections vanish due to the symmetry consideration.

In terms of the well-established 6×6 $\mathbf{k}\cdot\mathbf{p}$ approximation of Dresselhaus, Kip and Kittle [2],

$$L \equiv E_{xx}^{|x\rangle 2} \ , \ M \equiv E_{yy}^{|x\rangle 2} = E_{zz}^{|x\rangle 2} \ , \ N \equiv E_{xy}^{|x\rangle 2} \ ,$$

Table 1.2: Valence band parameters of the $\mathbf{k} \cdot \mathbf{p}$ theory for silicon and germanium.

Parameters	Unit	Si	Ge
L	eV·Å^2	-25.51	-143.32
M	eV·Å^2	-15.17	-22.90
N	eV·Å^2	-38.10	-161.22
Q	eV·Å^4	-125.0	
Δ	eV	60.044	0.282
a	eV	2.1	2.0
b	eV	-1.5	-2.2
d	eV	-3.4	-4.4
a_0	Å	5.4309	5.6561
c_{11}	10^{11}dyn/cm^2	16.56	12.853
c_{12}	10^{11}dyn/cm^2	6.39	4.826

the valence-band Hamiltonian matrix for the unstrained crystal is in the form

$$H_{\mathbf{k}\cdot\mathbf{p}} = \begin{vmatrix} H & 0_{3\times3} \\ 0_{3\times3} & H \end{vmatrix},$$

$$H = \begin{vmatrix} Lk_x^2 + Mk_{yz}^2 & Nk_xk_y & Nk_xk_z \\ Nk_yk_x & Lk_y^2 + Mk_{zx}^2 & Nk_yk_z \\ Nk_zk_x & Nk_zk_y & Lk_z^2 + Mk_{xy}^2 \end{vmatrix}, \quad (1.17)$$

where $k_{ij}^2 = k_i^2 + k_j^2$, $0_{3\times3}$ is the 3×3 zero matrix, L, M, N are band parameters.

The spin-orbital interaction matrix is described by the following matrix [3]

$$H_{\text{so}} = \frac{\Delta}{3} \begin{vmatrix} 0 & -i & 0 & 0 & 0 & 1 \\ i & 0 & 0 & 0 & 0 & -i \\ 0 & 0 & 0 & -1 & i & 0 \\ 0 & 0 & -1 & 0 & i & 0 \\ 0 & 0 & -i & -i & 0 & 0 \\ 1 & i & 0 & 0 & 0 & 0 \end{vmatrix}. \quad (1.18)$$

The values of parameters L, M, N and Δ for silicon and germanium are listed in Table 1.2 [2] for low values of $\mathbf{k}$ (low hole energy).

Eq. (1.17) includes only terms in k_ik_j. For high hole energies (high $\mathbf{k}$ values), terms of higher order in k_i must be included. In the first order approximation we assume that $E_{xxxx}^{\alpha 4} = Q$ is independent of $|\alpha\rangle$ and

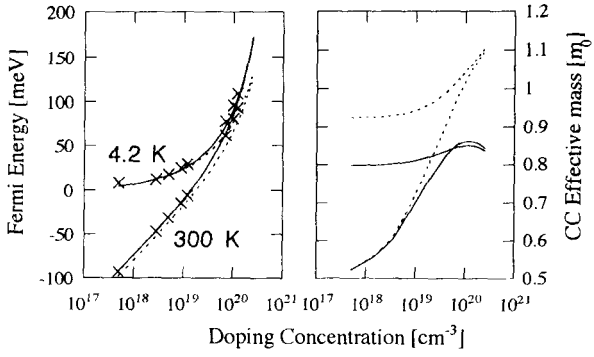

Figure 1.4: The Fermi energy and carrier-concentration effective mass as functions of the doping concentration for p-type silicon. Dashed lines are results without quartic terms, while the solid lines are the results of the modified $\mathbf{k}\cdot\mathbf{p}$ theory when $Q = -125\,\text{eV}\cdot\text{Å}^4$. Crosses mark the experimental data. (*After Fu and Willander, Phys. Lett. vol.A234, p.483-7, 1997.*)

$E^{\alpha 4}_{ijmn} = 0$ if i, j, m and n are not the same so that

$$H = \begin{vmatrix} Lk_x^2 + Mk_{yz}^2 + Qk_x^4 & Nk_xk_y & Nk_xk_z \\ Nk_yk_x & Lk_y^2 + Mk_{zx}^2 + Qk_y^4 & Nk_yk_z \\ Nk_zk_x & Nk_zk_y & Lk_z^2 + Mk_{xy}^2 + Qk_z^4 \end{vmatrix}. \tag{1.19}$$

Here parameter Q is to be determined by comparing calculated energy band structure with experimental measurement results.

In Table 1.3 and Fig. 1.4 we present results of Fermi energy and carrier-concentration effective mass (in the unit of free electron mass m_0) as functions of the doping concentration together with the measurement data from Ref. [4]. It is observed here that the introduction of the quartic terms significantly improves the description of the valence band structure at high hole energy. (We shall define the concepts of carrier-concentration effective mass and density-of-states (DOS) effective mass in the next sub-section.) The top of the heavy hole band is set as the zero reference energy, the calculation results are presented in such a way that the higher the hole energy, the deeper the energy level lies inside the valence band.

The introduction of the quartic terms modifies very much the description of valence band structure in the high hole energy range, thus resulting in the changes of the Fermi energy and the DOS effective mass as functions of doping concentration and temperature shown in Fig. 1.5 and Fig. 1.6 to compare the band structures calculated with and without quartic terms. It is observed here that the HH band is largely modified by the quartic terms.